Mendeleev Communications

Mendeleev Commun., 2025, **35**, 79–81

Formation of the Me_2SAuCl complex in the reaction of $HAuCl_4$ with quercetin in dimethyl sulfoxide

Stella A. Golovanova,[a] Anatolii P. Sadkov,[a] Gennady V. Shilov,[a] Tatyana A. Savinykh[a] and Alexander F. Shestakov*[a,b]

[a] *Federal Research Center of Problems of Chemical Physics and Medicinal Chemistry, Russian Academy of Sciences, 142432 Chernogolovka, Moscow Region, Russian Federation. E-mail: a.s@icp.ac.ru*

[b] *Department of Fundamental Physical and Chemical Engineering, M. V. Lomonosov Moscow State University, 119991 Moscow, Russian Federation*

DOI: 10.71267/mencom.7536

The reaction of quercetin with $HAuCl_4$ in a DMSO–water medium yields the oxidation products of the organic substrate along with the $(Me_2S)AuCl$ complex. According to quantum chemical modeling, the driving force of the process is the transfer of the oxygen atom from the initially formed complex $(Me_2SO)AuCl$ to the organic substrate.

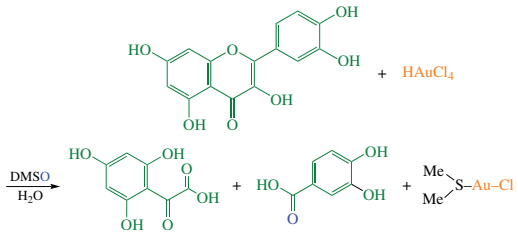

Keywords: quercetin, oxidation, gold complexes, dimethyl sulfoxide, dimethyl sulfide, DFT, modeling.

Quercetin **Qc** and $HAuCl_4$ are the components of a catalytic system with which methane is hydroxylated with atmospheric oxygen under mild conditions.[1] Previously,[2] using high-resolution NMR technique we discovered that in a DMSO–water (4 : 1) medium there occurred stoichiometric two-electron oxidation of quercetin with the aurate ion into a *p*-quinone methide derivative, which was then rapidly converted into semiketal **A** upon the addition of a water molecule (Scheme 1). The *p*-quinone methide has been identified in a number of studies[3] as an intermediate when implementing the antioxidant properties of **Qc**.

In aqueous solutions, even with excess **Qc** in the reaction, gold nanoparticles are quickly formed; the products of deep oxidation of quercetin such as CO and CO_2[4] are formed due to the disproportionation of intermediate Au^I compounds.[5] In the presence of DMSO, the formation of nanoparticles is suppressed, apparently due to the stabilization of the resulting Au^I complexes upon coordination with DMSO.

Under anaerobic conditions the reaction between quercetin and $HAuCl_4$ at an equimolar ratio is practically complete within

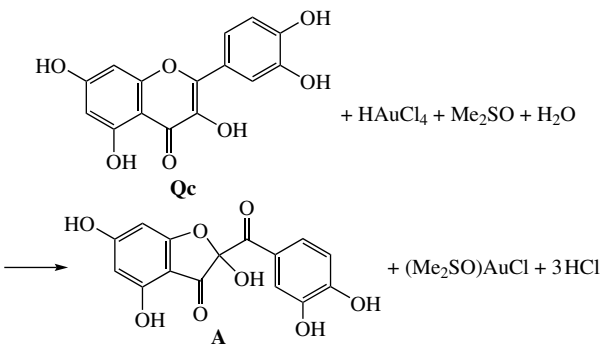

Scheme 1 *Reagents and conditions*: **Qc**, $HAuCl_4$, DMSO/H_2O (4 : 1 v/v), 20–22 °C, 24 h.

24 h. In this case, the characteristic absorption peak of **Qc** at 475 nm disappears, and it can be considered that quercetin is completely converted into semiketal **A** (see Online Supplementary Materials, Figure S1). Upon subsequent pumping out of the solvent, after a long time, the formation of colorless crystals was observed.†

The aim of this work was to clarify the chemical nature of this crystalline compound and the mechanism of its formation. The X-ray analysis‡ showed that, contrary to expectations, these crystals are not the only organic product of the stoichiometric reaction of two-electron oxidation, but the known[6] $(Me_2S)AuCl$ complex. Due to its good solubility, a significant proportion of it remains in the mother liquor containing organic components, so the yield of the crystalline form was 50%. The source of the Me_2S ligand in this compound is obviously DMSO, which also

† *Preparation of* $(Me_2S)AuCl$. Quercetin (Sigma), chlorauric acid ($HAuCl_4$) (Sigma), dimethyl sulfoxide (DMSO) (Tathimfarmpreparat), and double-distilled water were used in the work. The complex was obtained in a mixture of two solvents DMSO/H_2O (4 : 1 v/v). A stoichiometric amount of $HAuCl_4$ solution was added dropwise at room temperature (20–22 °C), with stirring, to a freshly prepared 2×10^{-1} M solution of **Qc**. Stirring was continued for another 2 h in a place protected from light. The next day, the reaction mixture was centrifuged to remove the precipitate. The complex was isolated by lyophilization in vacuum. Vacuum sublimation was carried out slowly over 2 weeks. The resulting viscous solution was stored in an inert atmosphere until crystals precipitated, which were washed and dried. The resulting product was transparent needle-shaped crystals, the yield was approximately 50%.

‡ *Crystal data for* $(Me_2S)AuCl$. The resulting single crystals were examined on an Agilent XCalibur single-crystal diffractometer with an EOS detector at a temperature of 200 K. The cell parameters $a = 6.0178(4)$, $b = 14.7644(8)$ and $c = 6.3374(4)$ Å, $V = 560.08(6)$ Å^3, and the spatial group $P2_1/c$ were determined. The crystal structure of $(Me_2S)AuCl$ was determined, which was characterized previously.[6]

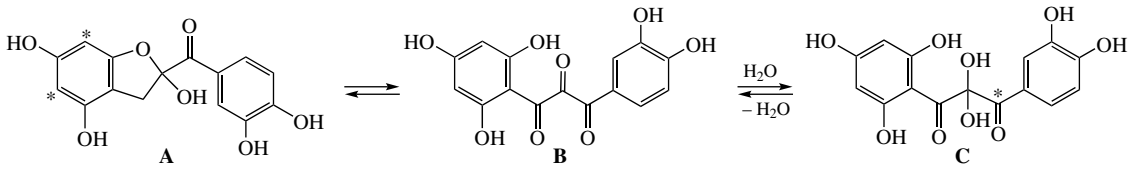

Scheme 2

acts as an oxidizing agent and a donor of the O atom. This means that after the formation of the *p*-quinone methide in the system, a slower process of its oxidation occurs. In blank experiments in an inert atmosphere, the spectra of quercetin solutions in DMSO practically did not change within one day, and only after 1 month a slight decrease in the bioflavonoid content was observed (Figure S2). Thus, Au^{I} complexes truly participate in the oxidation of semiketal **A**.

Quantum chemical modeling[§] was carried out to understand the mechanism of the oxidation process. The strictly identical value of H/D exchange[2] in the primary oxidation product **A** in positions 6 and 8, marked with asterisks* in the diagram, means the presence of a quickly established equilibrium of semiketal **A** with its isomer **B** with an open five-membered ring (Scheme 2). According to calculations, the addition of a water molecule to **B** to form ketal **C** occurs with an energy gain of 4.9 kcal mol^{-1}. However, taking into account entropy losses in this process, the equilibrium is shifted towards **B**.

Gold(I) usually forms linear complexes, and the coordination of DMSO through the S atom in the $(Me_2SO)AuCl$ complex is more favorable by 4.7 kcal mol^{-1}. When the O atom is removed from the Me_2SO molecule, the binding energy of the organic ligand to the AuCl fragment increases by 5.6 kcal mol^{-1}. In the case of transfer of this O atom to the C atom, marked with an asterisk* in structure **C**, simultaneous acceptance of a proton from the neighboring hydroxy group occurs and the final product **D** is formed (Scheme 3 and Figure S3) with a gain of 78.3 kcal mol^{-1}. Dimer **D** contains hydrogen bonds between the carboxy derivatives of pyrocatechol and phloroglucinol, typical oxidation products of quercetin.[7,8] However, the transition state (see Figure S3) of the direct oxidation reaction has a very high energy, 36.9 kcal mol^{-1}, relative to the non-interacting reagents **C** + $(Me_2SO)AuCl$, so this route is unrealistic at room temperature. On the other hand, it should be taken into account that during the primary oxidation reaction of quercetin, the acidity of the medium increases due to the formation of HCl. Therefore, it is necessary to consider the reactivity of the protonated form of **C**. In the case of protonation of the carbonyl

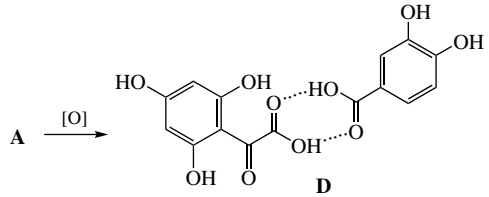

Scheme 3

[§] *Quantum chemical calculations*. Calculations were performed using the density functional PBE[9] and the extended basis: Au [10s6p6d5f5g] C, S, Cl [6s3p3d1f], H[5s1p] for valence electrons and SBC pseudopotential.[10] The Hirschfeld method[11] was used to calculate atomic charges. The nature of the transition states found was established by scanning the reaction coordinate in different directions, as well as by studying the forms of vibrations with an imaginary frequency. The search was carried out by the method of successive approximations using the optimization of suitable structures with fixed key distances. All calculations were carried out using the PRIRODA[12] software package at the computing facilities of the Joint Supercomputer center of RAS.

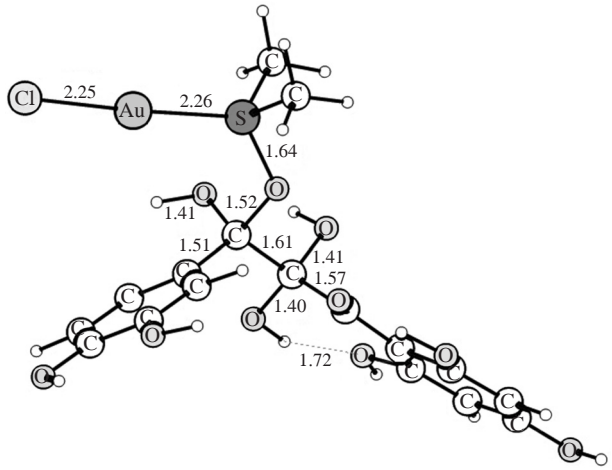

Figure 1 Structure of the adduct between the protonated species **C** and $(Me_2SO)AuCl$.

group C*O, a carbocation is formed, which attacks the nucleophilic O atom of the $(Me_2SO)AuCl$ complex. The adduct formed in this process (see Figure 1) has an energy higher by 6.0 kcal mol^{-1} relative to the reagents.

The transition state of adduct formation **TS1** (Figure 2) is located ~1 kcal mol^{-1} higher in energy, and the decomposition of the adduct into final oxidation products (Figure S4) is accompanied by a gain of 77.7 kcal mol^{-1} and requires overcoming a small activation barrier of 7.1 kcal mol^{-1}. The structure of the transition state **TS2** of the decay is shown in Figure 2.

The $\mathbf{C} \cdot H^+$ cation can form several types of hydrogen-bonded complexes with $(Me_2SO)AuCl$ (Figure S4). The most stable of them is formed with a gain of 19.9 kcal mol^{-1} and has a strong hydrogen bond of 2.01 Å between the Cl atom of the ligand and the protonated carbonyl group. This complex is the pre-reaction complex, as it was shown by the analysis of the reaction coordinate of the adduct formation. A similar complex, in which the O atom of the DMSO ligand participates instead of the Cl atom in the hydrogen bond, is located by 3.4 kcal mol^{-1} higher. A very short O···H hydrogen bond of 1.44 Å, apparently, is an obstacle to its transformation into the adduct with the minimum activation energy. An isomeric complex with a longer hydrogen bond of 1.87 Å between the O atom of the DMSO ligand and the adjacent OH group (see Figure S4) is closer in energy to the adduct, but it is also not pre-reaction. The energy diagram of the oxidation reaction between $(Me_2SO)AuCl$ and the protonated ketal **C**, proceeding *via* the formation and decomposition of the adduct, is shown in Figure S5.

In the crystal structure of $(Me_2S)AuCl$, chains with short Au–Au contacts of 3.187 Å are formed (Figure S6) due to aurophilic interactions, the energy of which in the model complexes $[(Me_2S)AuCl]_2$ and $[(Me_2S)AuCl]_3$ is 11.2 and 9.3 kcal mol^{-1}, respectively. The energy of aurophilic interaction in the dimer $[(Me_2SO)AuCl]_2$ is a comparable value of 11.0 kcal mol^{-1}.

Figure 3 shows the molecular structure of trimer $[(Me_2S)AuCl]_3$. The bond lengths calculated by the PBE method are in fairly good agreement with the experimental data. The replacement of the Me_2S ligand with Me_2SO or H_2O in the

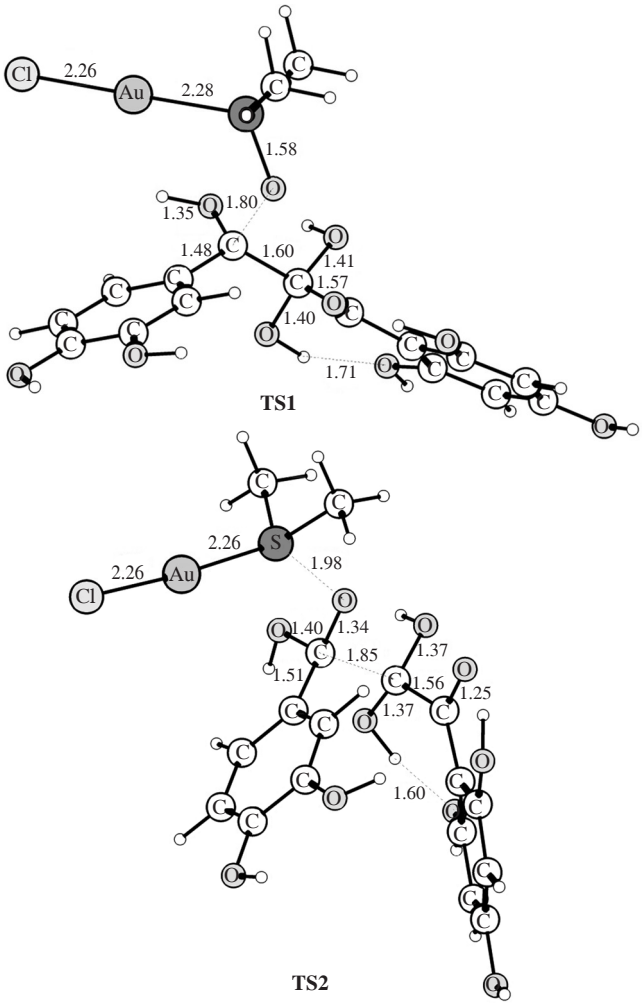

Figure 2 Transition states of adduct formation from the pre-reaction complex (**TS1**) and its decomposition (**TS2**).

$(Me_2S)AuCl$ complex is energetically unfavorable by 5.6 and 21.2 kcal mol^{-1}, respectively. This is the driving force behind its formation as Me_2S accumulates in the system as a result of the oxidation of the *p*-quinone methide.

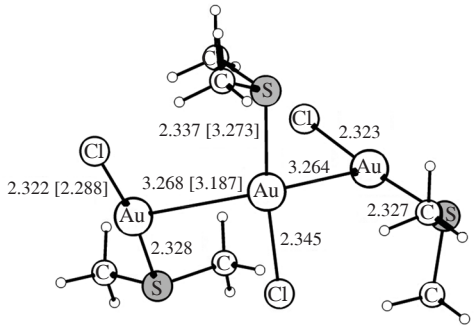

Figure 3 Structure of the trimeric structural unit of the $(Me_2S)AuCl$ complex according to calculation data. Experimental data are given in square brackets.

When the O atom is detached from the Me_2SO ligand, the energy of its binding to the AuCl fragment increases by 5.6 kcal mol^{-1}. This circumstance can be considered as the driving force for the formation of the $(Me_2S)AuCl$ complex as a result of the exothermic oxidation reaction of semiketal **A**. The possible process of replacing the Me_2S ligand with an H_2O molecule is energetically unfavorable by 21.2 kcal mol^{-1}.

To summarize, the obtained experimental and theoretical data show that the oxidation of quercetin with $HAuCl_4$ in a water–DMSO mixture does not end at the stage of stoichiometric two-electron oxidation and ultimately leads to the destruction of the intermediate semiketal **A**. This process takes place due to the enhancement of the oxidative properties of the DMSO ligand in the $(Me_2SO)AuCl$ species formed in the first stage and is followed by crystallization of the $(Me_2S)AuCl$ complex.

This work was supported by the Ministry of Science and Higher Education of the Russian Federation (state registration no. AAAA-A19-119071190045-0).

Online Supplementary Materials

Supplementary data associated with this article can be found in the online version at doi: 10.71267/mencom.7536.

References

1 L. A. Levchenko, N. G. Lobanova, V. M. Martynenko, A. P. Sadkov, A. F. Shestakov, A. K. Shilova and A. E. Shilov, *Dokl. Chem.*, 2010, **430**, 50; https://doi.org/10.1134/S0012500810020059.
2 A. F. Shestakov, A. V. Chernyak, N. V. Lariontseva, S. A. Golovanova, A. P. Sadkov and L. A. Levchenko, *Mendeleev Commun*., 2013, **23**, 98; https://doi.org/10.1016/j.mencom.2013.03.016.
3 V. Krishnamachari, L. H. Levine and P. W. Paré, *J. Agric. Food Chem.*, 2002, **50**, 4357; https://doi.org/10.1021/jf020045e.
4 A. F. Shestakov, S. A. Golovanova, N. V. Lariontseva, A. P. Sadkov, V. M. Martynenko and L. A. Levchenko, *Russ. Chem. Bull.*, 2015, **64**, 2477; https://doi.org/10.1007/s11172-015-1180-3.
5 A. M. Bondžić, T. D. Lazarević-Pašti, B. P. Bondžić, M. B. Cŏlović, M. B. Jadranin and V. M. Vasić, *New J. Chem.*, 2013, **37**, 901; https://doi.org/10.1039/C2NJ40742F.
6 P. G. Jones and J. Lautner, *Acta Crystallogr.*, 1988, C**44**, 2089; https://doi.org/10.1107/S0108270188009151.
7 J. S. Barnes and K. A. Schug, *J. Agric. Food Chem.*, 2014, **62**, 4322; https://doi.org/10.1021/jf500619x.
8 I. G. Zenkevich, A. Yu. Eshchenko, S. V. Makarova, A. G. Vitenberg, Yu. G. Dobryakov and V. A. Utsal, *Molecules*, 2007, **12**, 654; https://doi.org/10.3390/12030654.
9 J. P. Perdew, K. Burke and M. Ernzerhof, *Phys. Rev. Lett.*, 1996, **77**, 3865; https://doi.org/10.1103/PhysRevLett.77.3865.
10 W. J. Stevens, H. Bash and M. Krauss, *J. Chem. Phys.*, 1984, **12**, 6026; https://doi.org/10.1063/1.447604.
11 F. L. Hirshfeld, *Theor. Chim. Acta*, 1977, **44**, 129; https://doi.org/10.1007/BF00549096.
12 D. N. Laikov, *Chem. Phys. Lett*., 1997, **281**, 151; https://doi.org/10.1016/S0009-2614(97)01206-2.

Received: 11th June 2024; Com. 24/7536